Influence of intermediate low-temperature heating on precipitation in nonstoichiometric GaAs

© *L.A. Snigirev*[1], *N.A. Bert*[1], *V.V. Preobrazhenskii*[2], *M.A. Putyato*[2], *B.R. Semyagin*[2], *V.V. Chaldyshev*[1]

[1] Ioffe Institute,
194021 St. Petersburg, Russia
[2] Rzhanov Institute of Semiconductor Physics, Siberian Branch, Russian Academy of Sciences,
630090 Novosibirsk, Russia

E-mail: leonidsnigirev17@gmail.com

Initial stage of precipitate formation during post-growth annealing of nonstoichiometric GaAs and GaAs$_{0.97}$Sb$_{0.03}$ grown by low-temperature (150°C) MBE on GaAs (001) substrate with intermediate growth interruption and simultaneous heating up to 250°C was studied by transmission electron microscopy. Short-term intermediate heating despite the low temperature was revealed to result in the precipitation of larger particles during subsequent post-growth annealing compared to the material not subjected to such heating. This effect is explained by the huge concentration of excess arsenic in LT-GaAs and LT-GaAs$_{0.97}$Sb$_{0.03}$ grown at 150°C, enhanced diffusion due to the high concentration of nonequilibrium gallium vacancies, and non-threshold nucleation.

Keywords: nonstoichiometric GaAs, LT-GaAs, precipitation.

1. Introduction

Epitaxial layers of gallium arsenide grown by molecular beam epitaxy (MBE) at low (usually 200−300°C) temperature (LT-GaAs) turn out to be non-stoichiometric as a result of the capture of excess arsenic, which is mainly embedded in the GaAs crystal lattice in the form of antisite defects As$_{Ga}$ with a concentration reaching $\sim 1\%$ [1]. Excess arsenic forms nanoscale crystalline precipitates semi-coherently embedded in the LT-GaAs matrix, and the material acquires a high resistivity (up to 10^8 Ohms·cm) and a sub-picosecond lifetime of charge carriers.

Due to such properties, LT-GaAs is used in insulating layers suppressing crosstalk in gallium arsenide integrated circuits with MOS-transistors [2]. Recently, interest in this material has increased again due to the prospects of its application for ultrafast photoresistive switches [3], emitters and receivers of terahertz radiation [4–7].

Growing of LT-GaAs layers at low temperatures is associated with the problem of disruption of epitaxial growth [8,9], which is due to the gradual coarsening of the growth surface as the thickness of the growing layer increases due to mismatch of the crystal lattice constants and suppression of migration of adatoms [10]. Usually, the critical thickness of the epitaxial layer, on which good crystal quality is preserved, is $\sim 1\,\mu m$ at an epitaxy temperature of 200°C, and it decreases significantly when using lower temperatures. This circumstance limits the possible applications of LT-GaAs with a strong deviation from stoichiometry, but with a low density of extended structural defects.

An intermediate interruption of growth is applied with a short-term ($\sim 10\,min$) increase in temperature to restore the

smoothness of the growth front, after which it again drops to the epitaxy temperature, and growth resumes [11,12]. In this way, it is possible to obtain relatively thick layers with low-temperature epitaxy of various materials. For LT-GaAs, it was found that the critical thickness of the growth disruption increases sharply when the temperature exceeds 240°C [9]. At the same time, it is believed that the precipitation of excess As begins with the annealing temperature ~ 400°C [13–15]. It seems that this opens up the possibility of using intermediate low-temperature (~ 250°C) heat treatment during epitaxial growth to increase the thickness of LT-GaAs layers without affecting the formation of nanoprecipitates during post-growth annealing.

This article presents the results of an experimental study of the effect of intermediate growth interruption with heating to a temperature of 250°C in the process of growing LT-GaAs and LT-GaAs$_{0.97}$Sb$_{0.03}$ on the characteristics of an ensemble of precipitates formed as a result of post-growth annealing.

2. Experiment procedure

Epitaxial layers of LT-GaAs and LT-GaAs$_{0.97}$Sb$_{0.03}$ were grown using the MBE method on a semi-insulating GaAs substrate with a surface orientation of $(001) \pm 0.5°$. Before deposition of the epitaxial layers, the substrate was heated to a temperature of 580°C to remove the protective oxide. Its desorption was tracked by changing the pattern of reflection high energy electron diffraction (RHEED) from diffuse scattering to distinct structural reflexes. The temperature was measured by a thermocouple built into the sample holder. The thermocouple readings were calibrated according to

known GaAs surface adjustment temperatures, which was also determined using RHEED. GaAs buffer layer with a thickness of $0.2\,\mu$m was grown after removal of the oxide on the substrate at the same temperature of 580°C. Then the temperature was reduced to 150°C, and the growth of the LT-GaAs or LT-GaAs layer$_{0.97}$Sb$_{0.03}$ began. Growth was stopped to prevent disruption of epitaxial growth with intermediate heating up to 250°C, which was carried out as soon as signs of diffuse scattering became significant in the RHEED pattern. The growth was interrupted by blocking the flux of gallium, while the epitaxial layer remained under the pressure of the arsenic flux. The time of temperature rise from 150 to 250°C was 5 min, the exposure interval at this temperature was controlled by the disappearance of the contribution of diffuse scattering in the RHEED pattern and lasted ~ 2 min. Then the growth temperature was returned to the initial value, which took about 10 min. A single interruption of growth with heating was required for LT-GaAs and a double interruption was required for LT-GaAs$_{0.97}$Sb$_{0.03}$ for obtaining a layer with a thickness of $1\,\mu$m. An epitaxial AlAs film with a thickness of 5 nm was deposited on the grown layer after reaching the specified thickness of $1\,\mu$m which serves as a diffusion barrier preventing As from evaporation during post-growth annealing. The growth ended with the deposition of a GaAs film of the same thickness to protect AlAs from oxidation.

The grown samples were divided into several parts, one of which was not annealed, and the others were annealed at temperatures of 400 or 600°C for 15 min in the growth chamber of the MBE installation under vapor pressure As$_4$.

Structural studies of the obtained epitaxial layers LT-GaAs and LT-GaAs$_{0.97}$Sb$_{0.03}$ were carried out by transmission electron microscopy (TEM) in a microscope JEM-2100F (JEOL, Japan) with an accelerating voltage of 200 kV. Electron-transparent samples for TEM were prepared in cross-section (110) by a commonly accepted procedure of mechanical grinding-polishing for initial thinning and finishing ion sputtering. Diffraction microscopy methods were used for the study both in the image mode with diffraction or phase contrast, and in the diffraction mode from the selected area.

3. Experimental results and discussion

Figure 1 shows an electron micrograph of a cross-section of an LT-GaAs sample subjected to post-annealing at a temperature of 400°C. The thickness of the epitaxial layer measured from the image is 950 nm. The dark contrast line observed in the LT-GaAs layer at a distance of 650 nm from the boundary with the GaAs buffer layer corresponds to the interruption of growth, as a result of which the growth surface was decorated with particles of residual atmosphere. The presence of foreign particles obviously led, due to heterogeneous nucleation, to the formation of larger As precipitates than in the volume of the layer where nucleation is homogeneous. Due to this it is possible to clearly identify
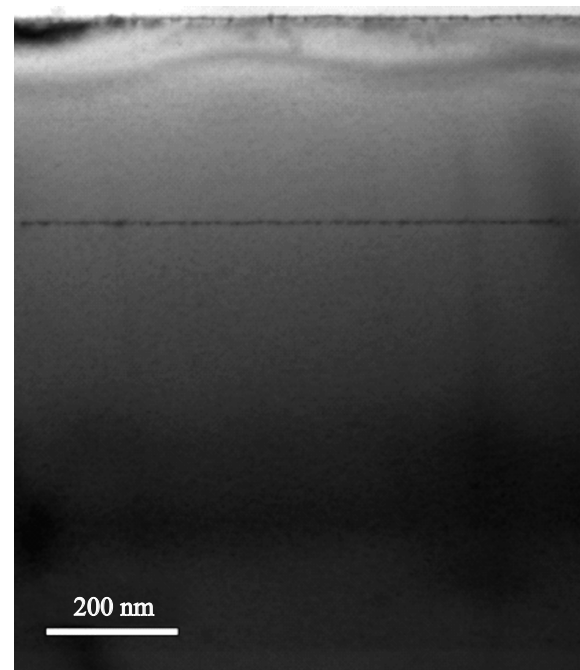
Figure 1. Bright-field image under two-beam conditions ($\mathbf{g} = 002$) of an LT-GaAs sample in cross section (110) after annealing at 400°C.
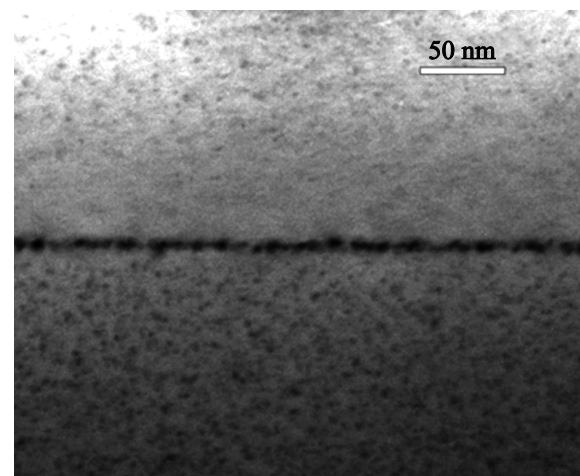
Figure 2. Magnified bright-field image under two-beam conditions ($\mathbf{g} = 002$) of a section of the LT-GaAs sample near the boundary separating the region with and without intermediate heating, after post-growth annealing at 400°C.

the areas of the layer that have been and have not been subjected to intermediate heating *in situ*.

Figure 2 shows an enlarged image of a section of the LT-GaAs layer near the boundary separating the region with and without intermediate heating, after post-post annealing at 400°C. Small precipitates formed, obviously, as a result of post-growth annealing at a relatively low temperature of 400°C are observed in the region above the

Parameters of the second phase particle ensemble in LT-GaAs$_{0.97}$Sb$_{0.03}$ after post-growth annealing at 400°C

Area	Medium size particles D_p, nm	Average volume particles V_p, nm^3	Concentration particles N_p, 10^{16} cm^{-3}	Volume fraction f, 10^{-3}
Upper	4.9	82	2.8	2.3
Medium	7	337	1.4	4.7
Lower	7.5	312	1.3	4.1
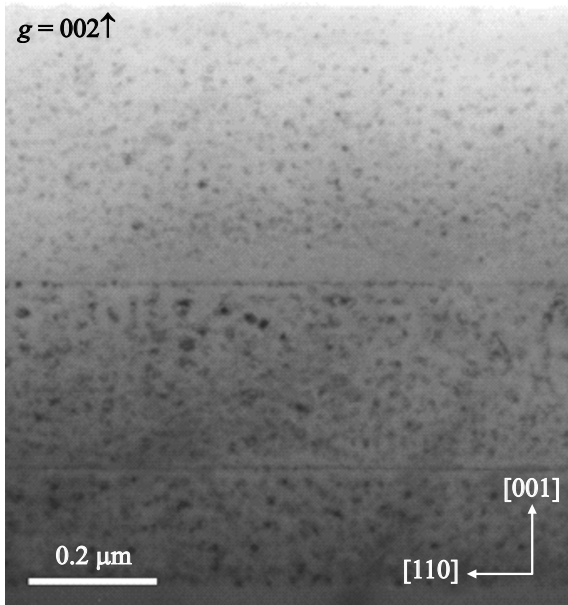
Figure 3. Bright-field image under two-beam conditions ($\mathbf{g} = 002$) of the LT-GaAs sample$_{0.97}$Sb$_{0.03}$ in cross section (110) after annealing at 400°C.

boundary not subjected to intermediate heating. It is also visually determined that in the area below the boundary, i.e. subjected to intermediate heating up to 250°C, the precipitates are larger and their concentration is higher than in the upper area, which was not subjected to such heating. Comparative statistical processing of the obtained images is difficult due to the small particle size. An estimate of the average size of precipitated precipitates gives a value of $1-2$ nanometers in the upper region and $1.5-3$ nanometers in the lower region.

A similar effect is more clearly observed in LT-GaAs$_{0.97}$Sb$_{0.03}$. The presence of antimony in a solid solution leads to the fact that it takes part in precipitation, and the formed particles turn out to be an alloy AsSb [16]. Figure 3 shows a TEM image of the cross-section of the LT-GaAs epitaxial layer$_{0.97}$Sb$_{0.03}$ grown with a double interruption of growth and heating to 250°C. It can be seen that the upper region of the layer which was not been subjected to intermediate heating contains smaller particles than the underlying regions that were subjected to a single (middle) or double (lower) heating.

More detailed images of the three regions of the epitaxial layer are shown in Figure 4. There are particles in the upper region not subjected to intermediate heating (Figure 4, a), whose size is distinctly smaller than in the lower regions that were subjected to single and double heating (Figure 4, b and c). Small dislocation loops are displayed near some particles in areas subjected to intermediate heating, which arise due to the relaxation of elastic stresses when the particle reaches a critical size of 8 nm [17].

The increased particle size allowed statistical processing of the obtained images, which gives an average size of D_p and an average volume of V_p particles. The thickness of the TEM lamella in each of the regions was measured using the electron diffraction method in a converging beam to determine the concentration of particles N_p. The obtained particle concentration values for the three regions are shown in the table. The volume fraction of the second phase particles f calculated from the measured values of the average volume V_p and concentration N_p is also indicated there.

The size and volume of particles in the area without intermediate heating are smaller than in the areas subjected to intermediate heating as follows from the values given in the table. At the same time, the concentration of particles in the upper region is about twice as high as in the lower ones. The volume fraction of particles in the upper region turns out to be significantly less than in the lower ones. This means that an increased concentration of anti-structural defects As$_{Ga}$ remains in the upper region which was not subjected to intermediate heating, compared with the lower regions that were subjected to such a procedure.

Thus, after post-growth annealing at 400°C, the regions of the LT-GaAs and LT-GaAsSb epitaxial layers subjected to intermediate heating at a low (250°C) temperature, at which it is assumed that excess arsenic precipitation does not occur, contain larger particles than areas grown without intermediate heating. Obviously, diffusion is activated in the process of intermediate heating despite low temperature and at least the nuclei of a new phase are formed. The diffusion in the GaAs cation sublattice where the antistructural defects As$_{Ga}$ are localized is known to occur by the vacancy mechanism [18,19]. The vacancy concentration V_{Ga} increases in LT-GaAs with decreasing growth temperature and it exceeds 10^{18} cm^{-3} at 200°C [20,21]. Since the effective diffusion coefficient of the vacancy mechanism is directly proportional to the vacancy concentration, it turns out to be many orders of magnitude higher than in the stoichiometric material [22–24]. At the same time, the
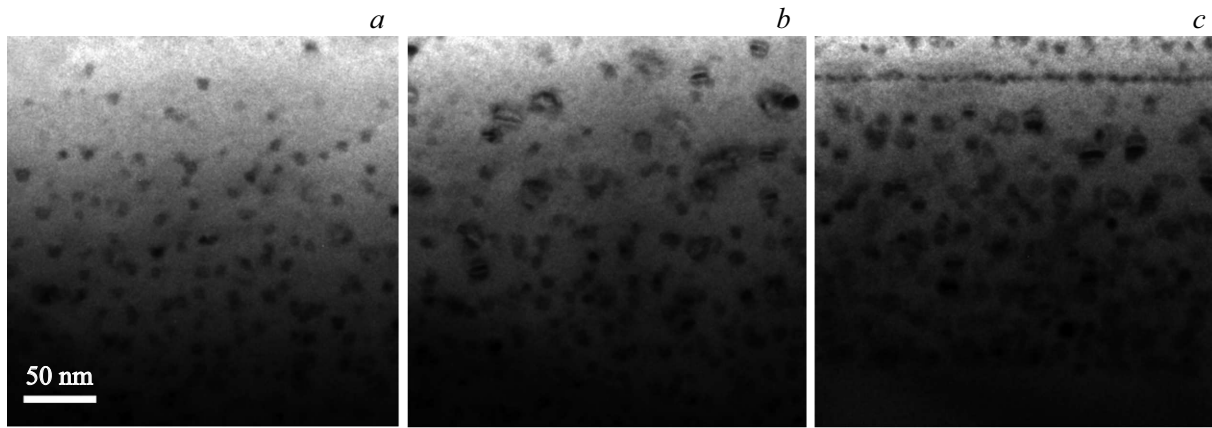
Figure 4. Enlarged bright-field images in two-beam conditions ($\mathbf{g} = 002$) of the upper (a), middle (b) and lower (c) regions of the LT-GaAs layer$_{0.97}$Sb$_{0.03}$ after post-annealing at 400°C.

diffusion is unsteady due to the gradual annihilation of nonequilibrium vacancies [25], and at the initial moment it is characterized only by the enthalpy of vacancy migration and is most enhanced, so that migration of As$_{Ga}$ is obviously activated even in case of a short-term heating to 250°C.

For the nucleus resulting from diffusion to be stable and continue to develop, its radius should be greater than the critical radius. As follows from the consideration of changes of internal energy during the diffusion decay of a supersaturated solution, the critical radius of the nucleus r^* can be estimated from the ratio

$$r^* = \frac{2\sigma v_a}{kT \ln S - E_{el}}, \qquad (1)$$

where σ — interfacial tension, v_a — atomic volume, S — supersaturation (the ratio of excess concentration to equilibrium). The elastic energy of nanoinclusion in the continuous medium approximation can be estimated as [26]

$$E_{el} = \frac{8\pi(1+v)}{3(1-v)} G \left(\frac{\Delta v_a}{v}\right)^{2/3} r^3, \qquad (2)$$

where G — shear modulus, v — Poisson's ratio, v_a/v — relative mismatch of atomic volumes in a particle and a matrix.

The contribution of elastic energy is insignificant for As precipitates in LT-GaAs due to the small discrepancy between the atomic volumes in the particle and in the matrix (0.0225 nm^3 for rhombohedral arsenic and 0.0226 nm^3 for GaAs). We use the experimental value of the surface tension of crystalline arsenic 260 MJ/m^2 to estimate the critical radius of the nucleus in a solid solution of As in GaAs [27]. The concentration of antisite defects [As$_{Ga}$] in LT-GaAs was determined in a sample annealed at 600°C, which leads to the complete precipitation of excess arsenic [16]. The initial content [As$_{Ga}$] is calculated as $1 \cdot 10^{20}$ cm^{-3} based on the average particle volume $V_p = 870$ nm^3 and their concentration $N_p = 5.9 \cdot 10^{15}$ cm^{-3}. A similar value is obtained for LT-GaAs$_{0.97}$Sb$_{0.0}$, where $V_p = 1400$ nm^3 and

$N_p = 4.2 \cdot 10^{15}$ cm^{-3}. Thermodynamically, the equilibrium concentration [As$_{Ga}$] can be estimated as

$$[As_{Ga}] = N_{Ga} \exp(-E_f/kT), \qquad (3)$$

where N_{Ga} — the concentration of atoms in the cation sublattice, and E_f there is an enthalpy of formation of an antisite defect. We obtain the equilibrium concentration As$_{Ga} \sim 10^7$ cm^3 using the enthalpy of formation As$_{Ga}$, which for semi-insulating GaAs is approximately 1.6 eV [28,29] for the heating temperature $T_h = 250$°C. As a result, the critical radius turns out to be < 0.15 nm, i.e. comparable to the interatomic distance. The same conclusion about the threshold-free formation of As nuclei in LT-GaAs follows from the simulation by the density functional method in the strong coupling approximation [30]. Due to the threshold-free formation, the resulting small cluster does not dissociate and continues to grow during subsequent post-formation annealing.

In the case of LT-GaAs$_{0.97}$Sb$_{0.03}$, Sb takes part in the formation of particles of the new phase, diffusing through the interstitial mechanism [31,32]. In addition to arsenic, antimony appears in the particle of the new phase, increasing the size of the precipitate. The additional elastic energy that occurs when antimony incorporates into the precipitate should increase the critical radius of the nucleus of the new phase, according to the formula (1). However, the contribution of the energy of elastic forces turns out to be insignificant with an exceptionally small size of the nucleus compared to the energy released during the phase transition. As a result, the generation of precipitates in LT-GaAs$_{0.97}$Sb$_{0.03}$, as in LT-GaAs, turns out to be a threshold-free process.

The occurrence of the nucleus is considered as a fluctuation process, and the mass precipitation of the dissolved substance is preceded by an incubation period, during which a stationary concentration of nuclei of critical size is achieved [33]. As a consequence, the mass growth of particles of the second phase in the region in epitaxial

LT-GaAs that was not subjected to intermediate heating is delayed in time during post-post annealing, and as a result, the precipitated particles are smaller in size than in the region that was subjected to intermediate heating, i.e., already subjected to the incubation period.

4. Conclusion

It was found as a result of electron microscopic studies that preliminary short-term heating of LT-GaAs or LT-GaAs$_{0.97}$Sb$_{0.03}$ to a relatively low temperature of 250°C, at which precipitation was not expected, leads to the formation of larger particles as a result of subsequent post-growth annealing at 400°C compared to the particles in the material not subjected to preheating. This effect is explained by the strong supersaturation of LT-GaAs and LT-GaAs$_{0.97}$Sb$_{0.03}$ grown at 150°C, enhanced diffusion due to the high concentration of nonequilibrium gallium vacancies and the threshold-free emergence of embryos. The impact of low-temperature treatment of LT-GaAs and solid solutions based on it should be taken into account when forming an ensemble of precipitates at the post-post annealing stage.

Conflict of interest

The authors declare that they have no conflict of interest.

References

[1] M.R. Melloch, J.M. Woodall, E.S. Harmon. Ann. Rev. Mater. Sci., **25**, 547 (1995).

[2] H. Thomas, J.K. Luo, D.V. Morgan, M. Lipka, E. Kohn. Semicond. Sci. Technol., **11**, 1333 (1996).

[3] C. Tannoury, M. Billet, C. Coinon, J-F. Lampin, E. Peytavit. Electron. Lett., **56** (17), 897 (2020).

[4] A. Jooshesh, F. Fesharaki, V. Bahrami-Yekta, M. Mahtab, T. Tiedje, T. Darcie, R. Gordon. Opt. Express, **25** (18), 22140 (2017).

[5] E.A. Prieto, A.D.L. Reyes, V.D.A. Vistro, N.I. Cabello, M.A. Faustino, J.P. Ferrolino, J.D. Vasquez, H. Bardolaza, J.P. Afalla, V.K. Magusara, H. Kitahara, M. Tani, A. Somintac, A. Salvador, E. Estacio. Appl. Phys. Express, **13**, 082012 (2020).

[6] Zhi-Chen Bai, Xin Liu, Jing Ding, Hai-Lin Cui, Bo Su, Cun-Lin Zhang. J. Mod. Opt., **68** (15), 824 (2021).

[7] O.M. Abdulmunem, K.I. Hassoon, J. Völkner, M. Mikulics, K.I. Gries, J.C. Balzer. J. Infr. Millim Terahertz Waves, **38**, 574 (2017).

[8] Z. Liliental-Weber, W. Swider, K. Yu, J. Kortright, F. Smith, A. Calawa. Appl. Phys. Lett., **58**, 2153 (1991).

[9] D.J. Eaglesham, L.N. Pfeiffer, K.W. West, D.R. Dykaar. Appl. Phys. Lett., **58**, 65 (1991).

[10] J. Herfort, V.V. Preobrazhenskii, N. Boukos, G. Apostolopoulos, K.H. Ploog. Physica E: Low-Dim. Syst. Nanostructur., **13** (2−4), 1190 (2002).

[11] D.J. Eaglesham. J. Appl. Phys., **77** (8), 15 (1995).

[12] A.E. Yachmenev, S.S. Pushkarev, R.R. Reznik, R.A. Khabibullin, D.S. Ponomarev. Progr. Cryst. Growth Charact. Mater., **66**, 100485 (2020).

[13] Z. Liliental-Weber, K.M. Yu, J. Washburn, D.C. Look. J. Electron. Mater., **22**, 1395 (1993).

[14] N.A. Bert, V.V. Chaldyshev, A.A. Suvorova, V.V. Preobrazhenskii, M.A. Putyato, B.R. Semyagin, P. Werner. Appl. Phys. Lett., **74** (11), 1588 (1999).

[15] I.S. Gregory, C. Baker, W.R. Tribe, M.J. Evans, H.E. Beere, E.H. Linfield, A.G. Davies, M. Missous. Appl. Phys. Lett., **83** (20), 4199 (2003).

[16] N. Bert, V. Ushanov, L. Snigirev, D. Kirilenko, V. Ulin, M. Yagovkina, V. Preobrazhenskii, M. Putyato, B. Semyagin, I. Kasatkin, V. Chaldyshev. Materials, **15**, 7597 (2022).

[17] V.V. Chaldyshev, N.A. Bert, A.E. Romanov, A.A. Suvorova, A.L. Kolesnikova, V.V. Preobrazhenskii, M.A. Putyato, B.R. Semyagin, P. Werner, N.D. Zakharov, A. Claverie. Appl. Phys. Lett., **80**, 337 (2002).

[18] U.M. Gösele, T.Y. Tan, M. Schultz, U. Egger, P. Werner, R. Scholz. Otwin Breitenstein. Def. Dif. Forum, **143−147**, 1079 (1997).

[19] D. Shaw. *Diffusion in Semiconductors* (Springer Handbook of Electronic and Photonic Materials, 2007).

[20] J. Gebauer, F. Börner, R. Krause-Rehberg, T.E.M. Staab, W. Bauer-Kugelmann, G. Kögel, W. Triftshäuser, P. Specht, R.C. Lutz, E.R. Weber, M. Luysberg. J. Appl. Phys., **87** (12), 15 (2000).

[21] M. Luysberg, H. Sohn, A. Prasad, P. Specht, Z. Liliental-Weber, E.R. Weber, J. Gebauer, R. Krause-Rehberg. J. Appl. Phys., **83**, 561 (1998).

[22] Y.K. Sin, Y. Hwang, T. Zhang, R.M. Kolbas. J. Electron. Mater., **20**, 465 (1991).

[23] J.S. Tsang, C.P. Lee, S.H. Lee, K.L. Tsai, C.M. Tsai, J.C. Fan. J. Appl. Phys., **79** (2), 664 (1996).

[24] N.A. Bert, V.V. Chaldyshev, Yu.G. Musikhin, A.A. Suvorova, V.V. Preobrazhenskii, M.A. Putyato, B.R. Semyagin, P. Werner. Appl. Phys. Lett., **74** (10), 1442 (1999).

[25] R. Geursen, I. Lahiri, M. Dinu, M.R. Melloch, D.D. Nolte. Phys. Rev. B, **60**, 10926 (1999).

[26] V.V. Chaldyshev, A.L. Kolesnikova, N.A. Bert, A.E. Romanov. J. Appl. Phys., **97**, 024309 (2005).

[27] D. Bouša, E. Otyepková, P. Lazar, M. Otyepka, Z. Sofer. Chem. Nano Mater., **6**, 821 (2020).

[28] A. Chroneos, H.A. Tahini, U. Schwingenschlogl, R.W. Grimes.
J. Appl. Phys., **116**, 023505 (2014).

[29] M. Jiang, H. Xiao, S. Peng, L. Qiao, G. Yang, Z. Liu, X. Zu.
Nanoscale Res. Lett., **13**, 301 (2018).

[30] T.E.M. Staab, R.M. Nieminen, M. Luysberg, Th. Frauenheim.
Phys. Rev. Lett., **95**, 125502 (2005).

[31] M. Schultz, U. Egger, R. Scholz, O. Breitenstein, U. Goesele,
T. Tan. J. Appl. Phys., **83**, 5295 (1998).

[32] N. Engler, H.S. Leipner, R.F. Scholza, P. Werner, U. Gosele.
Physica B: Condens. Matter, **308**–**310**, 742 (2001).

[33] M.P. Anisimov. Uspekhi khimii, 72 (7), 664 (2003) (in
Russian).

Translated by A.Akhtyamov